BMC Cancer

RESEARCH

Open Access

Heterogeneity of T cells regulates tumor immunity mediated by *Helicobacter pylori* infection in gastric cancer

Zhisheng Wu[1†], Xinya Wang[2,3†], Shujing Shi[4†], Deyuan Kong[3,5†], Chuanli Ren[6], Lijun Bian[7], Yuanliang Gu[7], Fangmei An[2,8], Qiang Zhan[2,8], Caiwang Yan[2,3,7], Chupeng Hu[3*], Yun Chen[1,2,3,5,9,3*], Runqiu Jiang[10*] and Jinfei Chen[11,12*]

Abstract

The impact of *Helicobacter pylori* (*H. pylori*) status on gastric cancer survival remains unclear. In this study, we conducted a prognostic analysis of 488 gastric cancer patients and performed single-cell RNA sequencing (scRNA-seq) on 18,717 T cells from six tumor samples with varying *H. pylori* statuses. Our findings revealed that gastric cancer patients with *H. pylori* infection had significantly longer survival times compared to those with negative *H. pylori* status. After unsupervised re-clustering of T cells based on scRNA-seq data, we identified ten $CD4^+$ and twelve $CD8^+$ clusters. Among them, four $CD8^+$ T cell clusters exhibited distinct distributions based on H. pylori infection status. One cluster, marked by *CXCL13*, showed high levels of *IFNG* and *GZMB* in *H. pylori*-infected patients, while another cluster, which expressed immune suppression related genes like *AREG* and *PTGER2*, was predominantly comprised of cells from non-infected patients. High *PTGER2* expression was significantly associated with worse prognosis in patients with high *CD8* expression. These insights advance our understanding of *H. pylori*'s influence on T cell responses in gastric cancer, aiding in treatment and prognostic strategies.

Keywords Gastric cancer, *Helicobacter pylori*, Immune microenvironment, Survival

†Zhisheng Wu, Xinya Wang, Shujing Shi and Deyuan Kong contributed equally to this work.

*Correspondence:
Chupeng Hu
hcpzzq15651677721@126.com
Yun Chen
chenyun@njmu.edu.cn
Runqiu Jiang
jiangrq@nju.edu.cn
Jinfei Chen
jinfeichen@sohu.com

[1]School of Chemistry and Chemical Engineering, Center of Interventional Radiology and Vascular Surgery, Nurturing Center of Jiangsu Province for State Laboratory of AI Imaging & Interventional Radiology, Department of Radiology, Medical School, Zhongda Hospital, Southeast University, Nanjing, Jiangsu, China
[2]Wuxi People's Hospital, Wuxi People's Hospital of Nanjing Medical University, Wuxi Medical Center, Wuxi, China
[3]Department of Immunology, Key Laboratory of Human Functional Genomics of Jiangsu Province, Nanjing Medical University, Nanjing, China
[4]Department of Rehabilitation, School of Sport and Health, Nanjing Sport Institute, Nanjing, China
[5]Jiangsu Key Lab of Cancer Biomarkers, Prevention and Treatment, Collaborative Innovation Center for Cancer Personalized Medicine, Nanjing Medical University, Nanjing, China
[6]Department of Laboratory Medicine, Clinical Medical College of Yangzhou University, Yangzhou, China
[7]Department of Epidemiology, Center for Global Health, School of Public Health, Nanjing Medical University, Nanjing, China
[8]Department of Gastroenterology, the Affiliated Wuxi People's Hospital of Nanjing Medical University, Wuxi, China
[9]Research center for clinical oncology, Jiangsu Cancer Hospital, the Affiliated Cancer Hospital of Nanjing Medical University, Nanjing, China
[10]Jiangsu Laboratory of Molecular Medicine, Medical School of Nanjing University, Nanjing, China
[11]Department of Oncology, the First Affiliated Hospital of Wenzhou Medical University, Wenzhou, China
[12]Zhejiang Key Laboratory of Intelligent Cancer Biomarker Discovery and Translation, First Affiliated Hospital, Wenzhou Medical University, Wenzhou, China

Introduction

Helicobacter pylori (*H. pylori*) has been classified as a Group I carcinogenic pathogen [1] because its infection is epidemically and etiological associated with the oncogenesis of gastric cancer (GC) [2]. Hence, it is well accepted that eliminating *H. pylori* infection is an effective way to prevent GC. However, GC develops through a multistep process, whether *H. pylori* play a carcinogenic role throughout this progression is controversial. Masanori summarized a hit-and-run mechanism that *H. pylori* is not required for the maintenance of a neoplastic phenotype in established cancer cells in which pro-oncogenic actions are successively taken over by a series of genetic and/or epigenetic alterations during long-standing *H. pylori* infection [3]. In addition, it is noteworthy that eradication of *H. pylori* appears to be ineffective for the prevention of GC in two trials that included subjects with precancerous lesions, including low to high-grade dysplasia at baseline [4, 5]. One reason for this may be that the elevated pH caused by *H. pylori* facilitates the intrusion of oral or intestinal bacteria into the stomach, which may additionally contribute to the development of mucosal lesions [6], while the damaged environment becomes unsuitable for *H. pylori* survival, especially in GC [7].

The gut microbiota and the immune system have coevolved and affect each other directly via metabolic crosstalk [8]. For example, Beura and colleagues [9] discovered that wild mice, pet store mice, and adult humans have a highly differentiated memory $CD8^+$ T-cell compartment in their blood, whereas "clean" laboratory mice and human neonates do not. Especially, multiple studies have provided strong evidence that immunotherapy may be an effective treatment for cancer if tumor microenvironment (TME) components are properly understood and judiciously targeted [10]. Phenotypic differences in T cell infiltration within the TME can be categorized into three types: "immune-inflamed", "immune-excluded", "immune-desert", depending on $CD8^+$T cells infiltration status [11]. Recently, Montalban-Arques et al. [12] confirmed that commensal *Clostridiales* strains could enhance the immunity and transform the TME from an "immune-desert" phenotype to an "immune-inflamed" phenotype by increasing the frequencies and activity of tumor-infiltrating IFN-γ^+CD8^+T cells, which ultimately improved the prognosis of colorectal cancer patients. In this context, it has been shown that the efficacy of cancer therapies depends on the composition of the microbiome [13].

In GC, there is no consensus regarding the foe or friend role of *H. pylori* infection in patients' prognosis. Georgios et al. [14] have reported that infection with *H. pylori* is associated with higher relapse-free survival and overall survival in patients who have curative resection without residual, local, or metastasized tumors. They speculated that cancer immunity might be suppressed in *H. pylori* negative patients, conversely, both innate and adaptive immunity have been significantly boosted due to *H. pylori* infection. Recently, a retrospective study has demonstrated that *H. pylori* infection prolongs survival in GC patients within the PD-L1-treated group [15]. However, the detailed mechanisms remain unknown.

Here, we aim to identify whether *H. pylori* infection contributes to the "immune-inflamed" TME, which immune cell components are responsible for building up such a TME, and how the differential immune cells influence the prognosis of GC patients. After performing a prognostic analysis of GC in Chinese population, we isolated intratumoral $CD45^+$ immune cells from human GC tissues with or without *H. pylori* infection and addressed these questions by analyzing *H. pylori*-specific immune cells through single-cell RNA sequencing. Our work enhances the understanding of heterogeneity between patients with different *H. pylori* infection status and provides a basis for individualized treatment for GC.

Materials and methods

Study population

Between 2006 and 2016, 1,198 consecutive patients with GC were recruited from the First Affiliated Hospital of Nanjing Medical University, Northern Jiangsu People's Hospital, and the Affiliated Hospital of Yangzhou University. All cases were newly diagnosed, with no prior treatment, including radiotherapy or chemotherapy. Each case was histopathologically or cytologically confirmed to have GC by at least two local pathologists. After signing informed consent, we collected 5 mL of venous blood from the patients and conducted a face-to-face interview concerning demographic data (e.g., age and sex) and lifestyle information (e.g., smoking and drinking) at the time of recruitment when available as previously described [16]. Furthermore, for patients who underwent curative resection, an independent reviewer assessed the following clinical information post-surgery: tumor size and localization; depth of tumor invasion; lymph-node metastasis; histological grading; and tumor type according to Laurén classification. The clinical stage was classified by the anatomical nodal site according to the 6th edition of the tumor-node-metastasis (TNM) classification.

All patients were followed up from the time of enrollment until death or the last follow-up (last follow-up: June 2019) every 6 months. The follow-up data included treatment information (chemotherapy or radiotherapy) and survival status (alive or dead, time of death, and cause of death). The latest medical records from their treating physicians were checked as a complement, and additional follow-up data were also obtained by contacting family physicians.

Definition of *H. pylori* infection status and the inclusion criteria

Based on the dataset, 207 patients were excluded from the study because they had metastatic disease or didn't underwent surgery ($n = 150$) and without any available follow-up data ($n = 57$). In order to ensure the accuracy of *H. pylori* infection status, patients without clinical records of urease or breath test results, which represents present infection of *H. pylori*, were further excluded ($n = 349$). After combing the results of serology assay for *H. pylori* infection which represents past infection of *H. pylori*, 76 patients were excluded due to lack of blood samples ($n = 35$) or hemolysis ($n = 41$). Then, patients with discordant results between urease or breath tests records and serology results were also excluded ($n = 78$). Only patients with positive results of both urease or breath tests records and serology tests were defined as *H. pylori* positive, while patients with negative results of both urease or breath tests records and serology tests were defined as *H. pylori* negative. Finally, a total of 488 patients who had both available follow-up and clinical information were enrolled, in which 264 patients were *H. pylori* positive and 224 were negative for *H. pylori* (Supplementary Fig. 1).

For single-cell RNA sequencing, the *H. pylori* infection status of gastric cancer tissues was determined intraoperatively using urease testing. Single-cell sequencing was subsequently conducted on samples obtained directly from the same region of the tested tissue, thereby ensuring a precise representation of the infection status. Finally, three *H. pylori*-positive and three *H. pylori*-negative individuals were included for single-cell RNA sequencing analysis (Supplementary Table 2).

Serology assay for *Helicobacter pylori* (*H. pylori*) infection

H. pylori infection status was determined using an *H. pylori* IgG ELISA kit (IBL International, Hamburg, Germany) according to the manufacturer's instructions. Briefly, plasma *H. pylori* IgG antibody was measured using 5 μL plasma and each sample was quantified using a calibration curve. Positivity was determined when the *H. pylori* IgG antibody titer of a sample was >10 U/ml. Individuals were regarded negative for *H. pylori* if they had no history of *H. pylori* infection on questioning and if they were also negative in the *H. pylori* IgG ELISA test. Sensitivity and specificity for the *H. pylori* IgG ELISA, as provided by the manufacturer, were 96.0% and 96.0%, respectively.

For further details regarding the materials and methods, please refer to the supplementary information.

Results

H. pylori infection was associated with better survival in Chinese gastric cancer patients

To examine the effect of *H. pylori* infection on the survival of GC, 488 patients were enrolled in the study and divided into two groups according to the *H. pylori* infection status (Supplementary Table 1). Among these patients, there were 372 men and 116 women, with a median age of 63 years. Of these, 224 were negative for *H. pylori* (hereafter referred to as "*H. pylori-*"), while the remaining 264 patients were positive for *H. pylori* (hereafter referred to as "*H. pylori+*"). Additionally, the *H. pylori+* group had a higher proportion of smokers and drinkers, whereas the proportion of patients with stage IV was relatively lower than that in the *H. pylori-* group.

As shown in Table 1, the median survival time was 36.33 months, and 190 patients (38.93%) died of GC in our cohort. The median survival time for *H. pylori+* patients was 142.3 months, compared to 82.1 months for *H. pylori-* patients (Fig. 1A, HR = 0.64, 95% CI = 0.48–0.85, $P = 2.35 \times 10^{-3}$). Additionally, we found that age, gender, clinical stage, and radiotherapy were significantly associated with the survival of our subjects with GC (Table 1; Fig. 1B and Supplementary Fig. 2). In multivariate analyses, we revealed that positive *H. pylori* status was significantly associated with a better prognosis for GC after adjusting for age, gender, clinical stage, and radiotherapy status. Furthermore, age and gender were also identified as prognostic factors for overall survival (Table 1). When adjusted for all variables in our study, only clinical stage and *H. pylori* status emerged as independent prognostic factors for survival. In this analysis, patients with positive *H. pylori* status had a significantly longer survival time compared to those with negative *H. pylori* status (Table 1, HR = 0.74, 95% CI = 0.55–0.99, $P = 0.045$).

Notably, for patients with early and intermediate stage GC (i.e., American Joint Committee on Cancer (AJCC) I, II and III), we observed a significant difference in overall survival between *H. pylori+* patients and *H. pylori-* patients ($P = 0.024$). However, no such association was found for patients with advanced cancer (i.e., AJCC IV, $P = 0.979$, Fig. 1C). Similar findings were noted when stratifying patients by other classifications for early and intermediate versus advanced disease. For instance, *H. pylori+* patients exhibited significantly higher survival rates than *H. pylori-* patients only among those with tumor depth not invading the visceral peritoneum or adjacent structures (i.e., T1, T2 and T3, $P = 0.030$, Supplementary Fig. 3A) and for those with nodal involvement of less than 2 (i.e., N0 and N1, $P = 4.43 \times 10^{-3}$, Supplementary Fig. 3B). Therefore, we identified *H. pylori* as an independent, beneficial prognostic factor, with the

Table 1 Univariate and multivariate analysis of predictive factors for overall survival in 488 patients with gastric cancer

Variables	Patients	Deaths	MST	HR (95% CI)	*P*	Adjusted HR (95% CI) [a]	Adjusted *P*[a]	Adjusted HR (95% CI) [b]	Adjusted *P*[b]
	N = 488	*N* = 190	(mo)						
Age									
< 63	244	83	133.3	1.00		1.00		1.00	
≥ 63	244	107	84.3	1.44 (1.08–1.92)	**0.012**	1.39 (1.04–1.86)	**0.025**	1.32 (0.98–1.78)	0.070
Gender									
Male	372	157	85.2	1.00		1.00		1.00	
Female	116	33	NA	0.64 (0.44–0.93)	**0.018**	0.68 (0.46–0.99)	**0.044**	0.64 (0.43–0.95)	**0.026**
Smoker									
No	324	123	101.3	1.00		1.00		1.00	
Yes	164	67	83.4	1.01 (0.75–1.36)	0.946	0.95 (0.70–1.31)	0.771	1.02 (0.68–1.54)	0.921
Drinker									
No	351	132	101.3	1.00		1.00		1.00	
Yes	137	58	83.4	1.02 (0.75–1.39)	0.905	0.89 (0.64–1.22)	0.458	0.88 (0.58–1.33)	0.536
Clinical stage									
AJCC I	102	10	NA	1.00		1.00		1.00	
AJCC II	71	21	142.3	2.69 (1.26–5.73)	**0.010**	2.52 (1.18–5.37)	**0.017**	2.61 (1.22–5.59)	**0.013**
AJCC III	137	63	83.4	5.19 (2.66–10.11)	$\mathbf{1.37\times10^{-6}}$	4.72 (2.41–9.24)	$\mathbf{6.00\times10^{-6}}$	4.92 (2.50–9.66)	$\mathbf{3.77\times10^{-6}}$
AJCC IV	178	96	30.2	13.77 (7.07–26.82)	$\mathbf{1.27\times10^{-14}}$	11.94 (6.09–23.40)	$\mathbf{1.27\times10^{-14}}$	12.56 (6.39–24.70)	$\mathbf{2.25\times10^{-13}}$
P trend				2.37 (1.98–2.84)	$\mathbf{<2.0\times10^{-16}}$	2.27 (1.89–2.72)	$\mathbf{<2.0\times10^{-16}}$	2.29 (1.91–2.76)	$\mathbf{<2.0\times10^{-16}}$
Chemotherapy									
No	183	65	NA	1.00		1.00		1.00	
Yes	305	125	88.0	1.06 (0.78–1.43)	0.713	0.81 (0.58–1.12)	0.200	0.81 (0.58–1.13)	0.212
Radiotherapy									
No	429	158	133.3	1.00		1.00		1.00	
Yes	59	32	63.7	1.73 (1.18–2.53)	$\mathbf{5.12\times10^{-3}}$	1.32 (0.90–1.95)	0.158	1.41 (0.94–2.12)	0.096
H. pylori									
Negative	224	100	82.1	1.00		1.00		1.00	
Positive	264	90	142.3	0.64 (0.48–0.85)	$\mathbf{2.35\times10^{-3}}$	0.74 (0.56-1.00)	**0.049**	0.74 (0.55–0.99)	**0.045**

[a]Adjusted for age, gender, clinical stage, radiotherapy status and *H. pylori* infection status

[b]Adjusted for age, gender, smoking, drinking, clinical stage, chemotherapy status, radiotherapy status and *H. pylori* infection status

H. pylori, *Helicobacter pylori*

effect being most pronounced in patients with early-stage cancer.

H. pylori affect gastric cancer mainly targeting CD8$^+$T cells within tumor microenvironment

It has been suggested that tumor-specific immune responses are upregulated in GC patients positive for *H. pylori* [14]. To evaluate the immunological mechanism of *H. pylori* in the GC microenvironment, we first explored the content of tumor-infiltrating lymphocytes (TILs) and found that CD3$^+$T cells were the dominant TIL population in both the *H. pylori*- and *H. pylori* + groups (Supplementary Fig. 4A). Given that CD8$^+$T cells play a pivotal role in clearing intracellular pathogens and tumors [17], we next examined the frequency of naive and memory subsets of CD3$^+$CD8$^+$T cells based on CD45RA and CCR7 expression. We found that effector memory T cells (T_{EM}, CD45RA$^-$CCR7$^-$) were the most prevalent subset, followed by central memory T cells (T_{CM}, CD45RA$^-$CCR7$^+$). Furthermore, the frequency of T_{EM} in *H. pylori* + GC was higher compared to *H. pylori*- GC (Supplementary Fig. 4B), indicating that *H. pylori* + GC generates a stronger immune response than *H. pylori*- GC (Supplementary Fig. 4C).

Single-cell transcriptomic profiling of the T cells in gastric cancer tumors among different *H. pylori* infection status

To elucidate the complexity of tumor-infiltrating T cells in GC in an unbiased manner, we conducted 3' droplet-based scRNA-seq (BD Rhapsody) on 18,717 flow-sorted CD3$^+$CD45$^+$T cells freshly isolated from three *H. pylori*- and three *H. pylori* + GC patients (Fig. 2A and Supplementary Table 2). T cell clusters were visualized using t-distributed stochastic neighbor embedding (t-SNE) following preprocessing, normalization and batch correction (Supplementary Fig. 5). Overall, we identified ten unique clusters based on their gene expression profiles, which included six distinct CD8$^+$T cell clusters and four

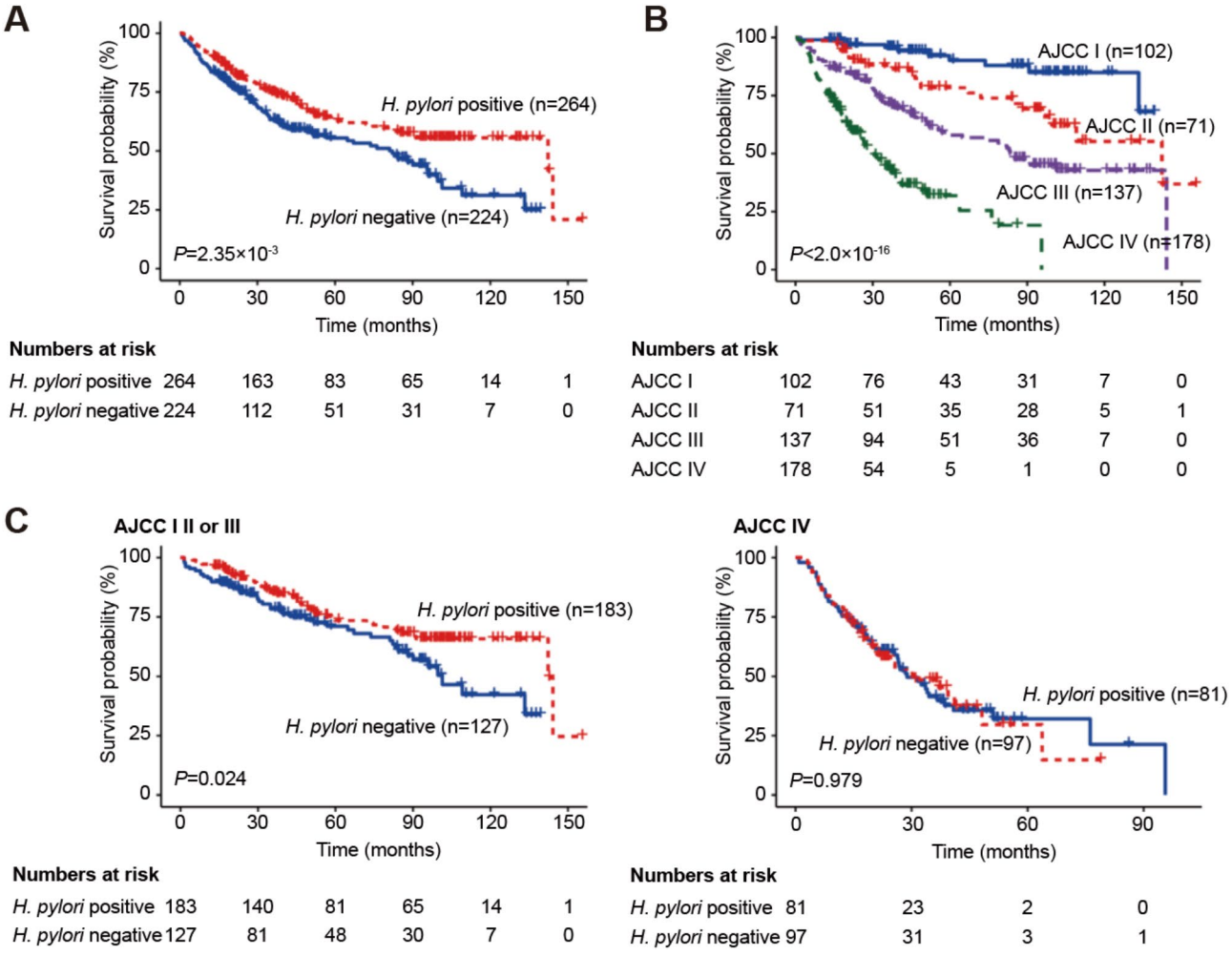

Fig. 1 *H. pylori* infection was associated with better survival in Chinese gastric cancer patients. **(A, B)** Kaplan-Meier survival curves for overall survival from 488 primary gastric cancer showing significant prognostic separation according to **(A)***H. pylori* infection and **(B)** clinical stage. **(C)***H. pylori* was an independent and beneficial prognostic factor pronounced in patients with early-stage cancer, not terminally stage cancer. *P*-value was calculated by the log-rank test

distinct CD4$^+$T cell clusters (Supplementary Fig. 6A-C). Each of these ten clusters harbored differentially expressed genes (DEGs) representing distinct cell types or subtypes (Supplementary Tables 3 and Supplementary Fig. 6D).

To address the intrinsic heterogeneity of T cells, we applied unsupervised re-clustering based on t-SNE and identified ten CD4$^+$ and twelve CD8$^+$ clusters (Fig. 2B, Supplementary Fig. 7). We further examined the expression and distribution of canonical T cell markers among these clusters (Fig. 2C, Supplementary Fig. 8). Among the ten CD4$^+$T cell clusters (Supplementary Table 4), we identified the CD4-C2-FOXP3, CD4-C3-TNFRSF4, CD4-C8-COL5A3, and CD4-C9-IFIT1 clusters, which represented regulatory T cells (Tregs) with high expression levels of *FOXP3*, *IKZF2* and *IL2RA*, as well as co-inhibitory molecules such as *TIGIT* and *CTLA4* (Fig. 2C, Supplementary Fig. 8A). Cells in the CD4-C5-CXCL13 and CD4-C6-TOX2 clusters exhibited high expression levels of *PDCD1* and *CXCL13* (Fig. 2C, Supplementary Fig. 8A), suggesting that they represent follicular T helper cells involved in the formation of ectopic lymphoid-like structures at inflammatory sites [18]. Two clusters of CD4$^+$T cells (CD4-C1-CCR7 and CD4-C7-FBLN7) were characterized by a gene signature that included *CCR7*, *LEF1*, *TCF7*, and *SELL* (Fig. 2C, Supplementary Fig. 8A), which are typical features of naive T cells. Notably, T cells from the CD4-C0-CCL5 and CD4-C4-SLC4A10 clusters exhibited high expression levels of *CD69*, which has been reported to be elevated in activated MAIT cells of patients with COVID-19 [19]. Given that MAIT cells can display effector functions involved in the defense against infectious pathogens [20], we found that the proportion of these two clusters were relatively increased in *H. pylori* + patients (Supplementary Fig. 8B), suggesting they may be activated by *H. pylori*.

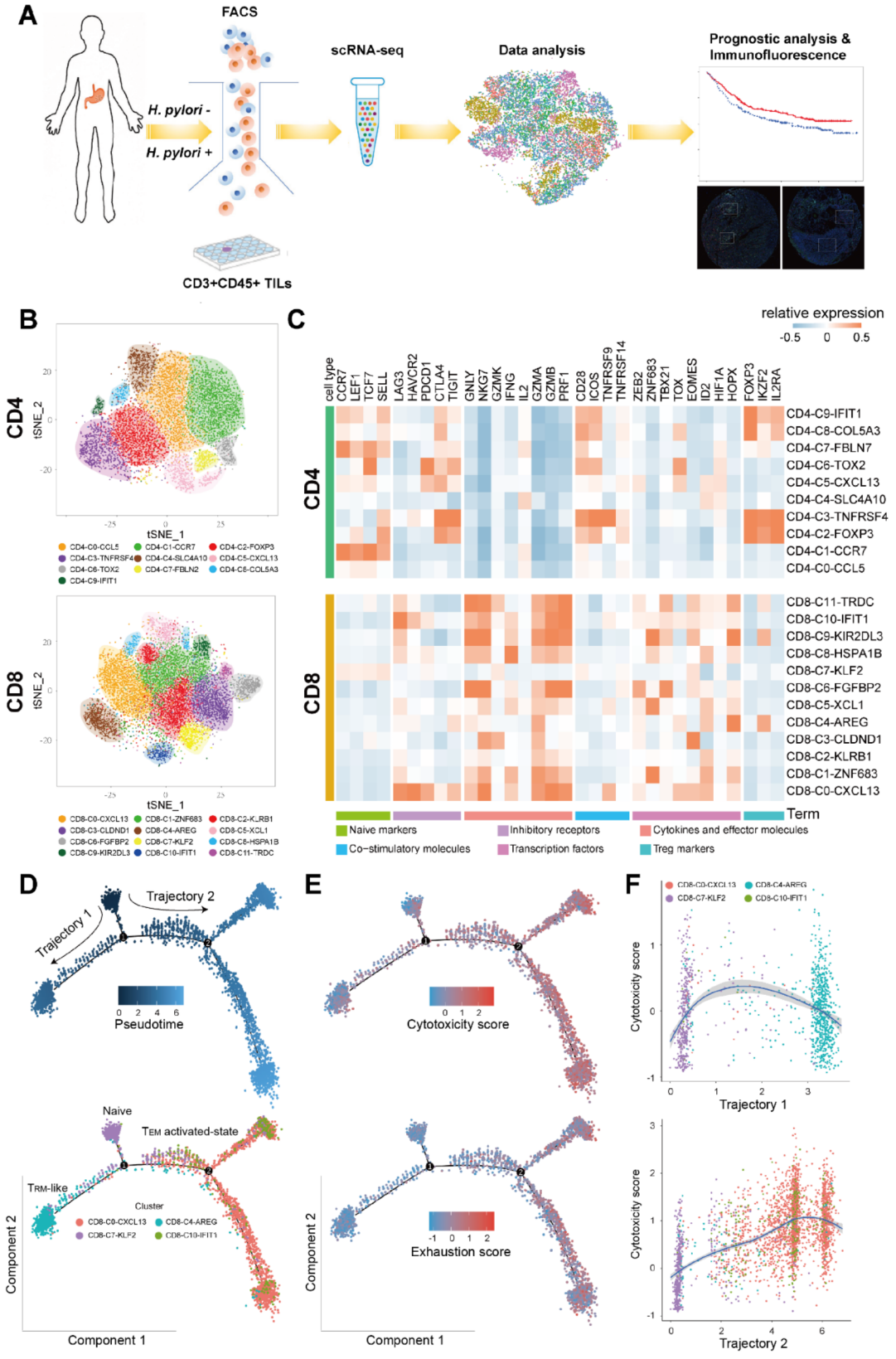

Fig. 2 (See legend on next page.)

(See figure on previous page.)

Fig. 2 Dissection and identifying infiltrated cell types in gastric cancer tissues. **(A)** Workflow showing the process of sample collection, single-cell dissociation, sorting, scRNA-seq, bioinformatic analysis and validation. **(B)** Re-clustering of $CD4^+$T cell and $CD8^+$T cells. **(C)** Average expression of selected T cell function-associated genes across different clusters. The box is proportional to the relative expression level of each gene. **(D)** The developmental trajectory of $CD8^+$T cells inferred by Monocle2. Each dot corresponds to one single cell, colored according to its cluster label. **(E)** Monocle components were correlated with functional features of $CD8^+$T cells, including scores of cytotoxicity and exhaustion calculated by the mean expression of gene sets related to T cell status (see Methods). **(F)** Significantly decreased or increased score of cytotoxicity in the differentiation process colored by cell clusters. The solid lines represent the relationship between the score with Monocle components

When focusing on the different $CD8A^+$ clusters (Supplementary Table 5), we observed that the CD8-C7-KLF2 cluster was characterized by a gene signature associated with naive T cells, including *CCR7*, *LEF1*, *TCF7*, and *SELL* (Fig. 2C, Supplementary Fig. 8C). Among the identified $CD8^+T_{EM}$, characterized by low expression of CCR7, we identified several distinct clusters: CD8-C0-CXCL13, CD8-C5-XCL2, CD8-C8-HSPA1B, and CD8-C10-IFIT1, which represent activated-state $CD8^+T_{EM}$ expressing effector molecules such as *IFNG*, *CCL4*, and *CCL5* (Fig. 2C, Supplementary Fig. 8C). Additionally, the CD8-C6-FGFBP2 cluster exhibited features of natural killer (NK) cells, expressing genes such as *NKG7*, *FGFBP2*, and *FCGR3A*; we refer to these cells as '$CD8^+T_{EM}$ NK-like' (Fig. 2C, Supplementary Fig. 8C). Interestingly, CD8-C0-CXCL13 and CD8-C10-IFIT1 also displayed variable expression of exhaustion markers such as *LAG3*, *HAVCR2*, and *PDCD1* (Fig. 2C, Supplementary Fig. 8C), indicating a potential activation-coupled exhaustion program possibly induced by both *H. pylori* infection and tumor cells.

Furthermore, cytotoxic $CD8^+$ T cells ($CD8^+T_{CYTOTOXIC}$) from the CD8-C1-ZNF683 and CD8-C9-KIR2DL3 clusters showed high expression levels of cytotoxicity-related genes such as *GNLY*, *GZMB*, *PRF1*, and tissue residency gene *ZNF683* (HOBIT) (Fig. 2C, Supplementary Fig. 8C). We also noted that the CD8-C4-AREG cluster exhibited expression of molecules suggestive of tissue-resident memory T cells (T_{RM}) with high expression of *ITGAE* (*CD103*), *ITGA1*, and *CD69*, while displaying low expression of *SELL*, *S1PR1*, and *KLF2* (Fig. 2C, Supplementary Fig. 8C), akin to T_{RM} cells described in humans and mice [21]. The CD8-C11-TRDC cluster was assigned to γδ-T cells, expressing *TRDC*, *TRGC1*, and cytotoxicity-associated genes, including *GNLY* [22], while the CD8-C2-*KLRB1* cluster was notable for high expression of *KLRB1*, recognized as hallmarks of mucosal-associated invariant T cells (Fig. 2C, Supplementary Fig. 8C) [23].

Unlike $CD4^+$T cells (Supplementary Fig. 8B), the clusters within $CD8^+$T cells exhibited distinct distributions. Notably, the CD8-C0-CXCL13 cluster predominantly comprised cells from *H. pylori* + patients, while the CD8-C4-AREG and CD8-C7-KLF2 clusters were almost exclusively populated by cells from *H. pylori*- patients (Supplementary Fig. 8D). We further analyzed the developmental trajectories of these differentially distributed cells using the Monocle 2 algorithm to establish a pseudotemporal ordering reflective of cell lineage. Given that the CD8-C7-KLF2 cluster is associated with naive T cells, we observed two major developmental trajectories (Fig. 2D), with T_{RM}-like and T_{EM} activated-state cells positioned at opposite ends of the pseudotemporal path, corroborating their distinct gene expression profiles. Additionally, we calculated cytotoxicity and exhaustion scores for each cell cluster. Along the trajectory, most $CD8^+$T cells exhibited progressively increasing cytotoxic activity, accompanied by a gradual rise in exhaustion levels (Fig. 2E). Notably, the cytotoxic activity score was downregulated in trajectory 1 toward the CD8-C4-AREG cluster, while it increased in trajectory 2 for both the CD8-C0-CXCL13 and CD8-C10-IFIT1 T cells (Fig. 2F), suggesting that these cells retained their ability for active division in the TME. Thus, single-cell analysis reveals that the $CD8^+$ population is heterogeneous with distinct subsets.

H. pylori infection promotes intratumoral immune activation with enhanced interaction between $CD8^+$T cells and epithelium

Focusing on the CD8-C0-CXCL13 cluster, we observed that, in addition to the high expression of *CXCL13*, this cluster specifically expressed genes such as *MYO7A*, *TOX*, and *PHLDA1* (Fig. 3A). We subsequently identified differentially expressed genes (DEGs) between the CD8-C0-CXCL13 group and the other groups. A total of 192 up-regulated and 118 down-regulated genes were detected in CD8-C0-CXCL13 T cells ($p.adj \leq 0.01$ and $|\log_2 FoldChange| \geq 0.25$) (Supplementary Fig. 9A and Supplementary Table 6). Gene ontology (GO) functional enrichment analysis revealed that the up-regulated genes in CD8-C0-CXCL13 T cells were enriched in signaling pathways related to T cell activation, regulation of lymphocyte activation, and regulation of T cell activation (Supplementary Fig. 9B). Additionally, KEGG analysis identified enrichment in crucial gene sets associated with anti-pathogen responses, including Th1 and Th2 cell differentiation, Th17 cell differentiation, as well as antigen processing and presentation (Supplementary Fig. 9C), which was potentially associated with *H. pylori* infection.

To further elucidate the molecular characteristics distinguishing CD8-C0-CXCL13 T cells in the context of *H. pylori* infection, gene set enrichment analysis (GSEA) was conducted. T cells from *H. pylori* + patients were found to be associated with cell activation involved in

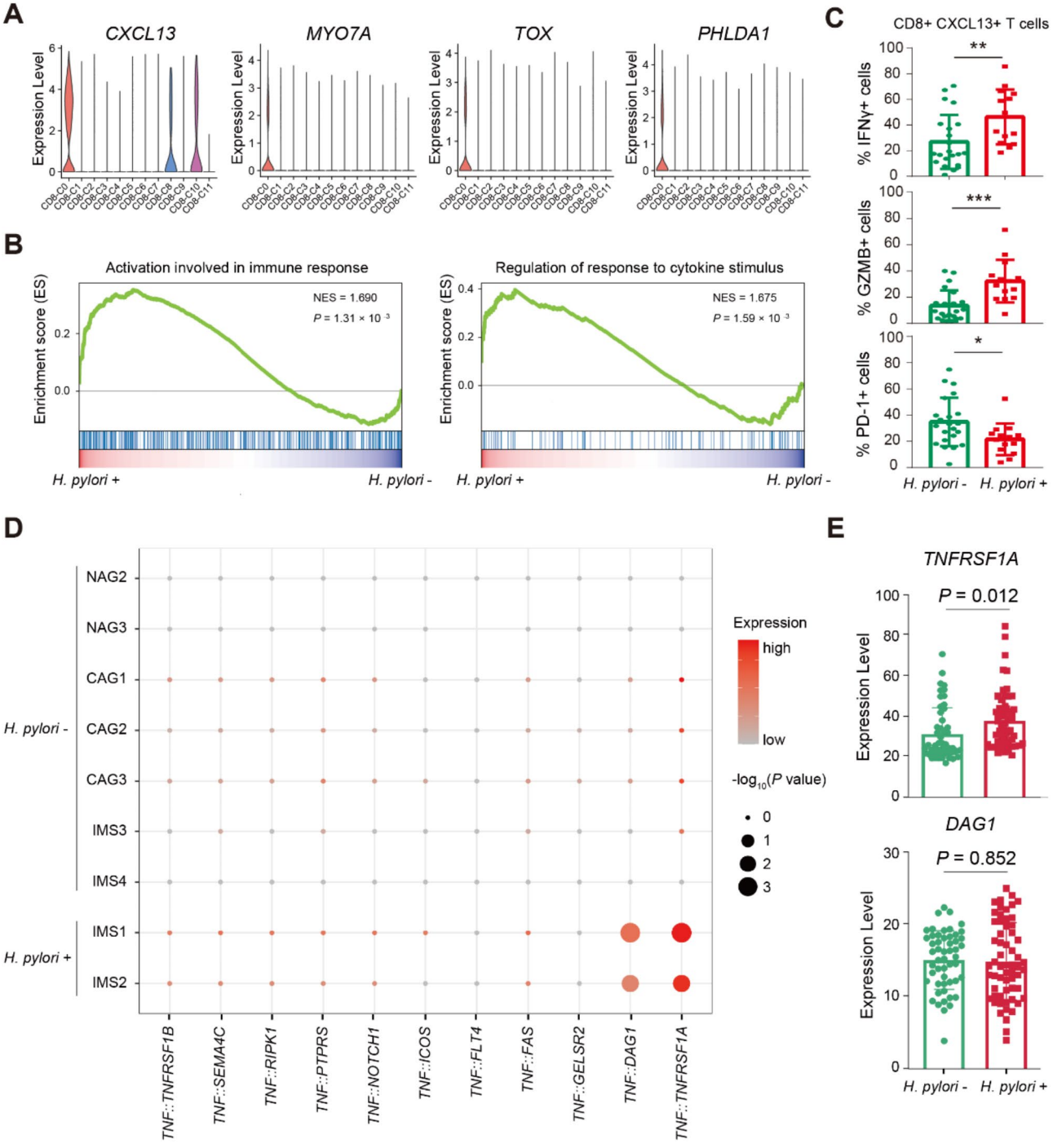

Fig. 3 Detailed characterization of T cells in CD8-C0-CXCL13 cluster with different *H. pylori* infection status. **(A)** Violin plots showing the expression levels of genes highly expressed in T cells of CD8-C0-CXCL13 cluster. **(B)** GSEA showing top enriched pathways in *H. pylori* + derived T cells. NES denotes normalized enrichment score. **(C)** Flow cytometry results showing that the expression levels of IFNγ and GZMB were upregulated, while PD1 level was downregulated in CXCL13^{+} CD8 T cells with *H. pylori*+. **(D)** Summary of selected ligand-receptor interactions between CD8^{+} T cells and epithelium. *P* values (permutation test) are represented by the size of each circle. The color gradient indicates the level of interaction. **(E)** Bulk RNA sequencing data from normal gastric mucosa tissues showing that the expression of *TNFRSF1A* was significantly increased in samples with *H. pylori* infection, while *DAG1* was not changed. *P* value was calculated with student's *t* test

immune response and regulation of response to cytokine stimulus, suggesting a potential protective role against local *H. pylori* infections (Fig. 3B). We then investigated the expression levels of various genes based on *H. pylori* infection status. Notably, we observed that cytotoxicity-associated genes, such as *IFNG* and *GZMB*, were upregulated in *H. pylori* + patients, while the expression of exhaustion marker *PDCD1* was downregulated (Supplementary Fig. 9D). Flow cytometry data corroborated these findings, revealing that the levels of IFN-γ and Granzyme B in $CD8^+CXCL13^+$T cell were significantly higher in *H. pylori* + patients compared to *H. pylori*- patients, whereas PD-1 expression exhibited the opposite trend (Fig. 3C). As expected, higher levels of *IFNG* and *GZMB* correlated with better prognosis in GC patients (Supplementary Fig. 9E, 9 F).

It is well-established that gastric epithelial cells from *H. pylori*-infected patients exhibit elevated levels of TNF receptors, which contribute to the activation of an adaptive immune response against invading infection. Utilizing dataset GSE134520, we evaluated TNF-dependent T cell functions in $CD8^+$T cells and epithelium. We found that the interaction between TNF and TNFRSF1A, as well as TNF and DAG1, was enhanced in the stomach with *H. pylori* infection (Fig. 3D), suggesting that such molecular interactions play a crucial role in generating an immune-activated TME in response to *H. pylori* infection. Notably, *TNFRSF1A*, rather than *DAG1*, exhibited a positive correlation with the $CD8^+$T cell signature and T_{EM} signature, while demonstrating a negative correlation with naïve T cells in the TCGA STAD cohort, as assessed using the TIMER2.0 webserver (Supplementary Fig. 9G). This indicates that *TNFRSF1A* may play an important role in promoting antitumor immunity against GC. Importantly, analysis of bulk RNA sequencing data from normal gastric mucosa tissues showed that the expression of *TNFRSF1A* was significantly increased in samples from *H. pylori*-infected patients, whereas *DAG1* levels remained unchanged (Fig. 3E). Collectively, our results suggest that *H. pylori* infection may recruit T cells into the tumor microenvironment through *TNFRSF1A-TNF* interaction, thereby enhancing immune activity.

As our data indicate that the CD8-C0-CXCL13 T cell is a highly prevalent effector subset within the GC microenvironment, we hypothesized that the single-cell-derived gene signature from the CD8-C0-CXCL13 cluster (Supplementary Table 5) would offer valuable prognostic information. Analysis of the available gene expression data revealed that the CD8-C0-CXCL13 signature was significantly associated with improved overall survival (Fig. 4A). Additionally, multicolor immunofluorescence staining demonstrated that both CXCL13 and CD103 were expressed in $CD8^+$T cells in the stroma and tumor tissues of *H. pylori*-infected samples (Fig. 4B), supporting the presence of these activated cells in GC.

T_{RM} cells marked by *PTGER2* worsen prognosis in *H. pylori* negative gastric cancer

Previous study has revealed that virus- or other pathogen-specific (bystander) $CD8^+T_{RM}$-like cells in tumors can be re-activated to induce antitumor immunity [24]. However, we identified 151 down-regulated genes in CD8-C4-AREG T cells (p.adj ≤ 0.01 and $|\log_2 FoldChange| \geq 0.25$) (Supplementary Fig. 10A and Supplementary Table 7), which were enriched in signaling pathways such as T cell activation, response to IFN-γ, and antigen processing and presentation (Supplementary Fig. 10B), indicating an immunosuppression state in CD8-C4-AREG T_{RM} cells. Although CD8-C4-AREG T_{RM} cells shared similar gene expression profiles between *H. pylori*- and *H. pylori*+ (Fig. 5A), GSEA analysis revealed that T cells from *H. pylori* + were associated with the inflammatory response and cytokine-mediated signaling pathways (Fig. 5B, Supplementary Fig. 10C). In contrast, the response to steroid hormone pathway was enriched in T cells from *H. pylori*- (Supplementary Fig. 10C), with increased expression levels of *AREG* and *PTGER2* (Fig. 5C). Further in vitro validation experiments also confirmed that *AREG* and *PTGER2* were down-regulated in the $CD8^+$T cells pulsed with *H. pylori* (Fig. 5D). Similarly, further immunohistochemistry staining also confirmed that AREG and PTGER2 were both inactivated by *H. pylori* infection in stroma and tumor tissues (Fig. 5E). Prognostic data from TCGA and GSE15459 show that the *PTGER2* can discriminate between patients with high *CD8* expression, with high *PTGER2* expression significantly associated with worse prognosis (Fig. 5F and Supplementary Fig. 10D). These data suggest that T_{RM} cells with high expression of *PTGER2* may serve as a therapeutic target to improve clinical outcomes in GC.

Discussion

Overall, we conducted a prognostic analysis of GC patients with different *H. pylori* infection statuses from a population level. Single-cell transcriptome profiling at the molecular level was performed, allowing for the characterization of different T cell subpopulations and *H. pylori*-activated clusters, as well as the delineation of transcriptional changes in *H. pylori*-activated T cells and the identification of co-stimulatory ligand expression in *H. pylori* + GC cells. The results of this study shed light on the mechanisms underlying target cell-dependent T cell responses induced by *H. pylori*, as well as the potential mechanisms underlying the responses of GC patients to *H. pylori* infection, and indicate that *PTGER2* may serve as a potential target for treating patients with GC.

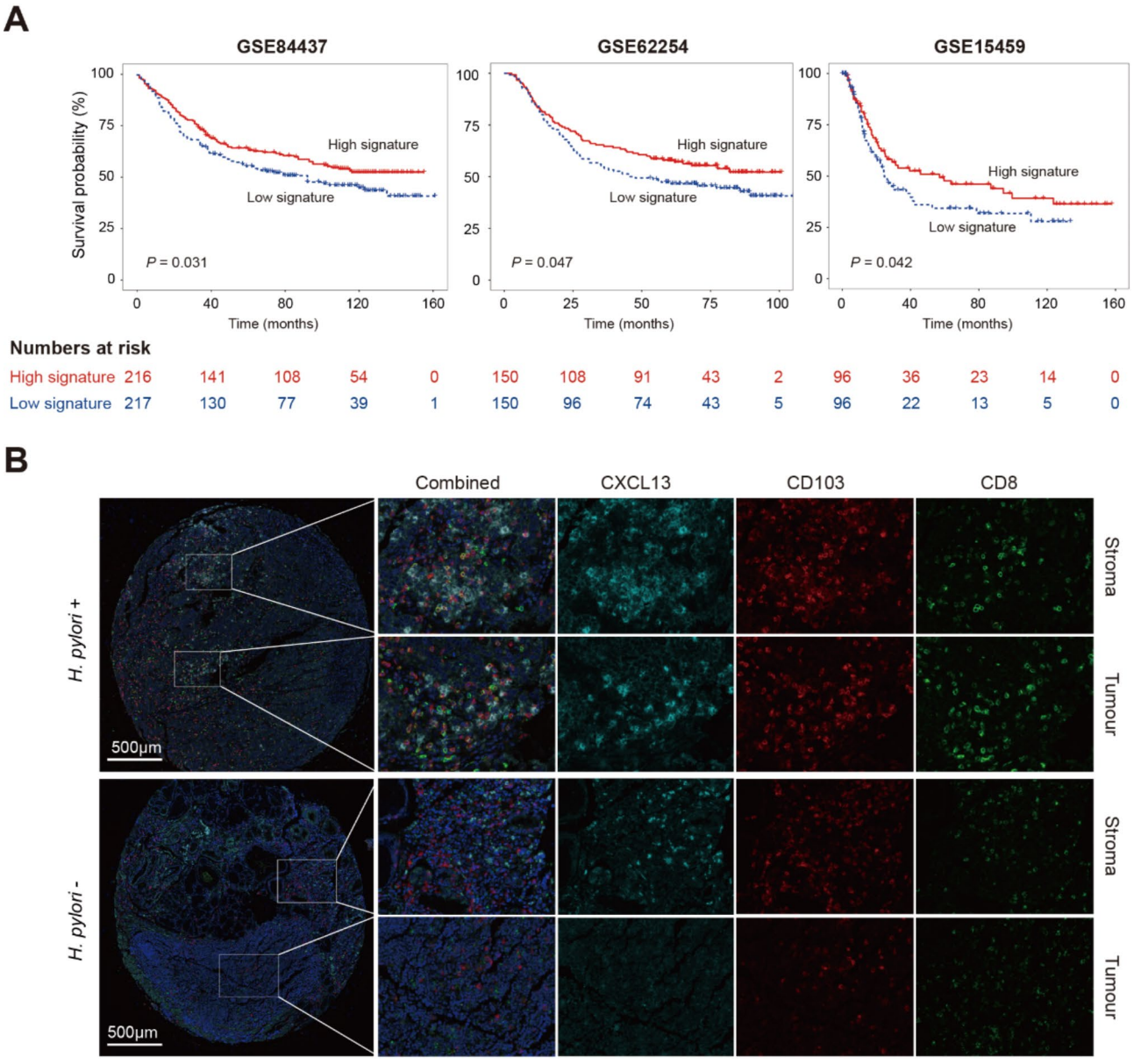

Fig. 4 Prognostic abilities of the gene signature derived from single-cell data of differentially expressed genes in CD8-C0-CXCL13 for human gastric cancers. **(A)** Overall survival for GC patients stratified according to CD8-C0-CXCL13 signature expression. *P*-value was calculated by the log-rank test. **(B)** The multicolor immunofluorescence staining of marker genes with CXCL13, CD103 and CD8 in stroma and tumor tissues between different *H. pylori* infection status

Although it is well established that *H. pylori* infection significantly contributes to the carcinogenesis of GC, the role of *H. pylori* infection in predicting the survival of GC patients is still less well understood. Interestingly, a prospective study has demonstrated that GC patients with positive *H. pylori* infection frequently showed better relapse-free survival and overall survival [14]. Recently, another study confirmed that *H. pylori* infection status is one of the most potentially important independent factors in predicting prolonged survival [15]. Additionally, other studies [25, 26], particularly a meta-analysis, have shown that *H. pylori* infection is an independent protective factor for GC progression, with this protective effect being consistent across different ethnic groups, *H. pylori* evaluation methods, and quality assessment measures [27]. In line with these results, our study also confirmed that *H. pylori* is an independent, beneficial prognostic factor, especially in patients with early-stage GC. This may be attributed to the fact that *H. pylori* infection is not the only factor affecting prognosis, and various therapies are available for advanced or relapsed GC patients [28].

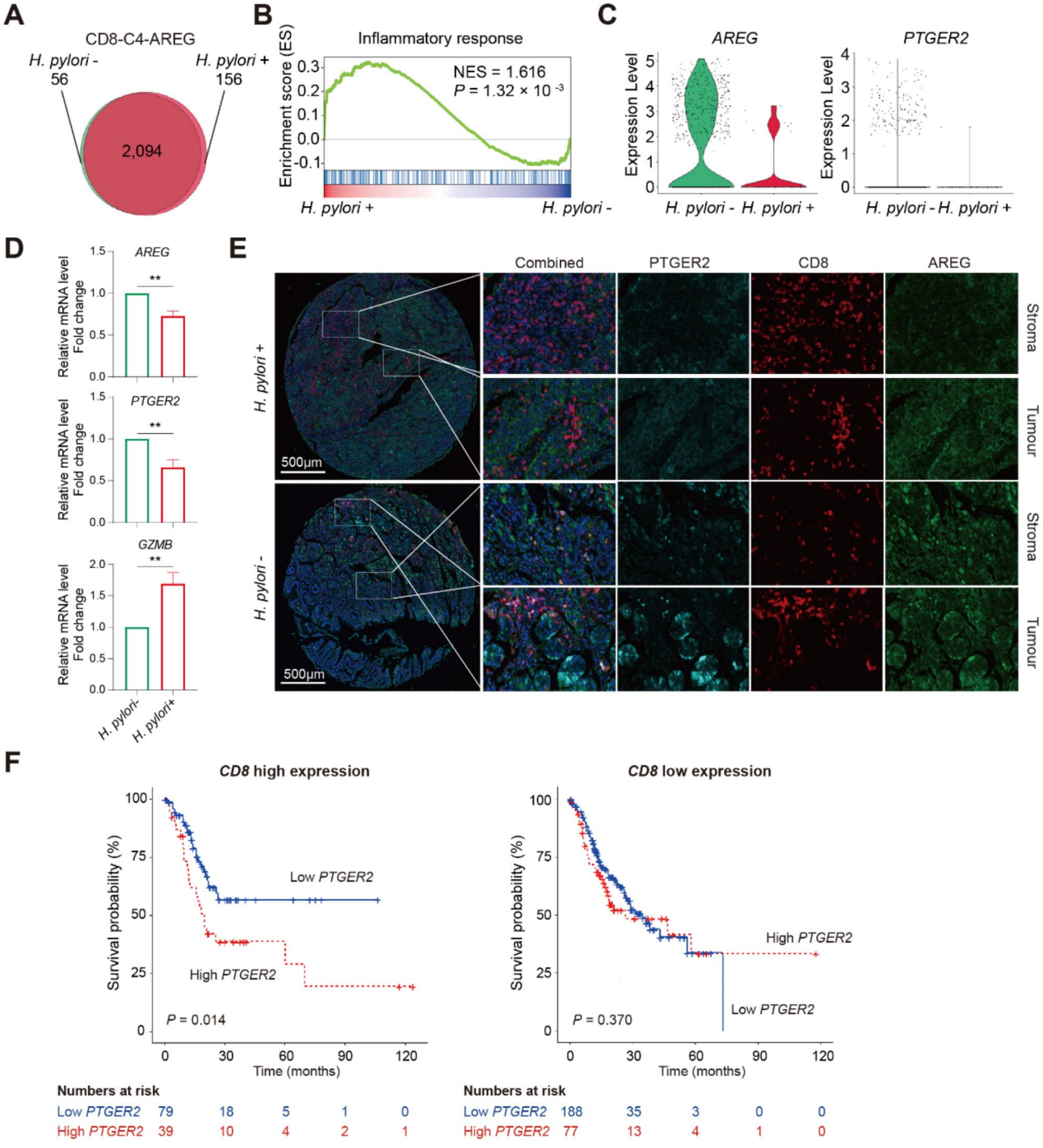

Fig. 5 T_{RM} cells marked by *PTGER2* worsen prognosis in *H. pylori* negative gastric cancer. **(A)** Venn diagram of shared and differentially expressed genes between T cells of CD8-C4-AREG cluster from patients with different *H. pylori* infection status. **(B)** GSEA showing enriched pathways in *H. pylori* + derived T cells. NES denotes normalized enrichment score. **(C)** Violin plots and corresponding dots showing that the expression levels of *AREG* and *PTGER2* were upregulated in T cells of CD8-C4-AREG cluster with *H. pylori*-. **(D)** Real-time PCR quantification of *AREG*, *PTGER2*, and *GZMB* expression in $CD8^+$T cells under control or following stimulation with *H. pylori*. The expression levels of each gene were normalized to *GAPDH* and then adjusted relative to the control group (served as 1). Data shown as mean ± SD. *P* value was calculated with student's *t* test. **(E)** The multicolor immunofluorescence staining of marker genes with PTGER2, CD8 and AREG in stroma and tumor tissues between different *H. pylori* infection status. **(F)** Overall survival for GC patients further stratified according to *PTGER2* expression within *CD8* expression strata from the TCGA database. *P*-value was calculated by the log-rank test

The suppressive effect of *H. pylori* on GC progression may be attributed to the induction of certain antitumor immune responses. The activation of T cells, the main immune effector cells for acquired immunity, is directly influenced by *H. pylori* bacterial products, such as VacA and arginase [29, 30]. Notably, Capitani et al. demonstrated that a specific *H. pylori* protein named HP1454 is a crucial bacterial factor that exerts its pro-inflammatory activity by directly modulating T-cell responses [31]. This finding prompted researchers to explore the mechanism of *H. pylori*-activated T cells in relation to the pathogenic factors of *H. pylori*. Additionally, several naturally occurring immunodominant $CD4^+$T cell responses in *H. pylori*-infected individuals have also been identified and characterized [32]. Although we did not observe significant differences among $CD4^+$T cells, we identified two clusters exhibiting distinct distributions of $CD8^+$T cells across different *H. pylori* infection statuses. Immunodominant T cells are believed to be more effective and play a central role in the host adaptive immunity against pathogens, as has been well demonstrated in various viral, bacterial, and tumor contexts [33]. Previous research has shown increased gastric T-cell infiltration in situ with a typical T-helper (Th)1 phenotype during *H. pylori* infection [34] and has identified several antigen-specific T-cell responses, such as HpaA-specific mucosal $CD4^+$T-cell responses with a Th1 profile, primarily occurring during the precancerous lesions stage [32]. However, in cancers, including GC, $CD8^+$T cells are essential for the immune eradication of cancer cells, although they often become dysfunctional over the course of tumorigenesis [35]. To address this issue, researchers have developed a series of immunotherapies, including immune checkpoint blockade [36], adoptive T cell therapy [37], and chimeric antigen receptor T cell therapy [38], to restore the functions of $CD8^+$T cells. Therefore, we speculate that these specific $CD8^+$T cells driven by *H. pylori* may contribute to the better prognosis observed in *H. pylori* + GC patients.

Recent technological advances have provided important insights into the heterogeneity of $CD8^+$TILs, demonstrating that distinct T cell subsets exist with different transcriptional programs and functional states [35]. When focusing on the CD8-C0-CXCL13 cluster, we noted that, in addition to the high expression of *CXCL13*, it also specifically expressed genes like *TOX*, a key transcription factor for $CD8^+$T cell differentiation during chronic viral infections and cancer [39], and *PHLDA1*, a required transcription factor for the regulation of the TLR-mediated immune response [40]. This indicates that these cells possess a strong immunological activity state. Consistent with the characteristic, pathway enrichment analysis revealed that the upregulated genes in CD8-C0-CXCL13 T cells were enriched for T cell activation pathways.

Since the epithelial cells are central to the cellular interaction network in GC [41], we evaluated the interactions between epithelial cells and matched $CD8^+$T cells. Tumor cells with high expression of *TNFRSF1A* may directly interact with TNF produced by $CD8^+$T cells, enhancing $CD8^+$T cell activity through the production of *GZMB* and *IFNG*, which suppresses tumor progression in GC with *H. pylori*. More importantly, a series of immune cell signatures have been identified by single-cell sequencing in various cancers, such as breast cancer [42], lung cancer [43], and melanoma [44], which were associated with patient prognosis. Similarly, we confirmed that CD8-C0-CXCL13 T cells may serve as key mediators of the improved clinical outcomes observed in human GC patients with *H. pylori* infection.

Recently, T_{RM} cells have been shown to both prevent and exacerbate various pathologies [45]. The involvement of T_{RM} cells in a range of malignancies makes the design of therapeutic strategies that can modulate either their production or activity an attractive goal. Additionally, further research has confirmed that T_{RM} cells display transcriptional features specific to individual tissues, allowing for their survival and long-term retention [46]. In this study, we identified a T_{RM} cell cluster marked by *AREG*, a member of epidermal growth factor family, and *PTGER2*, a receptor for prostaglandin E2, which was predominantly populated by cells that are *H. pylori*-negative. *AREG* has been shown to associate with type 2 immune-mediated resistance, tolerance mechanisms to infection, and immune suppression within the TME [47], while *PTGER2* enhances the pathogenic phenotype by regulating the balance of cytokines, such as IFN-γ/IL-10, in a context-dependent manner [48]. More importantly, previous studies have revealed that *PTGER2* is involved in tumor cell proliferation, invasion, and prognosis across various malignancies [49]. Here, we propose that high *PTGER2* expression is significantly associated with worse prognosis exclusively in patients with high *CD8* expression in GC. This finding suggests that T_{RM} cells exhibiting high *PTGER2* expression may represent a promising new prognostic factor and therapeutic target for anticancer therapies.

There are several limitations to the present study. First, to investigate the effect of *H. pylori* on the survival of patients with GC, we chose a longitudinal study design. However, because our data are derived from a single center, the results require further validation. Second, it remains uncertain whether *H. pylori* still exist in the cancer tissues of GC patients, which could lead to misclassification of *H. pylori* infection status. Additionally, we did not measure indicators such as antibody titers or other markers to assess the active status or quantity of *H. pylori* infection. Third, our focus was on TILs in GC, and we performed scRNA-seq of T cells. The ligand-receptor

interactions were inferred from a public database that primarily comprises normal tissues. To enhance the robustness and credibility of these inferences, further integration of scRNA-seq data from tumor cells and TME cells from GC patients, along with functional assays, would provide more compelling evidence. Fourth, due to the lack of immune-competent animal model for GC, the direct or indirect mechanisms involved in vivo remain unclear.

In summary, we utilized single-cell RNA sequencing to analyze the T cell landscape of GC patients, achieving high resolution regarding different *H. pylori* infection statuses. We identified two $CD8^+$T cell clusters: one consisting of activated $CD8^+T_{EM}$ cells, likely preceding activation by *H. pylori* and associated with better prognosis in GC, and the other comprised of T_{RM} cells, which were predominantly populated by *H. pylori*-negative cells and likely indicate exhaustion, correlating with worse prognosis in GC. Our findings provide valuable resources for deciphering the gene expression landscapes of heterogeneous cell types in GC and offer deep insights into cancer immunology for future drug discovery.

Conclusions

This study elucidates the molecular heterogeneity of tumor-infiltrating T cells in gastric cancer patients with different *Helicobacter pylori* (*H. pylori*) infection statuses. Through comprehensive single-cell RNA sequencing and functional analysis, we identified distinct $CD8^+$T cell clusters, including an activated $CD8^+$T cell cluster (CD8-C0-CXCL13) associated with improved patient survival and a tissue-resident memory T cell cluster (CD8-C4-AREG) linked to worse prognosis in *H. pylori*-negative patients. Our findings provide valuable insights into the complex interplay between *H. pylori* infection and the tumor immune microenvironment, highlighting potential targets for personalized immunotherapy in gastric cancer.

Abbreviations

H. pylori	*Helicobacter pylori*
GC	Gastric cancer
TNM	Tumor-node-metastasis
TME	Tumor microenvironment
TILs	Tumor-infiltrating lymphocytes
TEM	Effector memory T cells
TCM	Central memory T cells
MAIT	Mucosal associated invariant T cells
TRM	Tissue resident memory T cells
HR	Hazard ratio
CI	Confidence interval
MST	Median survival time
t-SNE	t-Distributed stochastic neighbor embedding
GO	Gene ontology

Supplementary Information

The online version contains supplementary material available at https://doi.org/10.1186/s12885-025-13957-9.

Supplementary Material 1
Supplementary Material 2
Supplementary Material 3
Supplementary Material 4
Supplementary Material 5
Supplementary Material 6
Supplementary Material 7
Supplementary Material 8
Supplementary Material 9

Acknowledgements

Not Applicable.

Author contributions

J.C., R.J., Y.C., and C.H. designed the study and edited the manuscript; Z.W., X.W., and S.S. performed statistical analysis and wrote the manuscript; Z.W., X.W., D.K., and C.Y. performed the experiments; C.R., L.B., Y.G., F.A., and Q.Z. participated in sample collection; J.C. had primary responsibility for final content.

Funding

This work was supported by grants from the National Natural Science Foundation of China (82125033, 82102876, and 82203226), the Key Research and Development Program of Jiangsu Province (BE2022770), the Jiangsu Science and Technology Project (BK20211039 and SBK2023022394), the Top Talent Support Program for young and middle-aged people of Wuxi Health Committee (BJ2023008), and the Natural Science Foundation of the Jiangsu Higher Education Institutions of China (21KJB320014). The funders had no role in the study design, data collection, data analysis, interpretation of data, or preparation of the manuscript.

Data availability

The data generated in this study are not publicly available due to information that could compromise patient privacy or consent but are available upon reasonable request from the corresponding author.

Declarations

Ethics approval and consent to participate

This study was approved by the institutional review board of Nanjing Medical University and adhered to the Declaration of Helsinki. All study participants provided written informed consent.

Consent for publication

Not Applicable.

Competing interests

The authors declare no competing interests.

Received: 19 November 2024 / Accepted: 17 March 2025
Published online: 28 March 2025

References

1. Schistosomes, liver flukes and Helicobacter pylori. IARC Working Group on the Evaluation of Carcinogenic Risks to Humans. Lyon, 7–14 June 1994. IARC monographs on the evaluation of carcinogenic risks to humans. 1994;61:1-241.
2. Malfertheiner P, Megraud F, O'Morain CA, Gisbert JP, Kuipers EJ, Axon AT, et al. Management of Helicobacter pylori infection-the Maastricht V/Florence consensus report. Gut. 2017;66(1):6–30.
3. Hatakeyama M. Helicobacter pylori CagA and gastric cancer: a paradigm for hit-and-run carcinogenesis. Cell Host Microbe. 2014;15(3):306–16.

4. Correa P, Fontham ET, Bravo JC, Bravo LE, Ruiz B, Zarama G, et al. Chemoprevention of gastric dysplasia: randomized trial of antioxidant supplements and anti-helicobacter pylori therapy. J Natl Cancer Inst. 2000;92(23):1881–8.
5. Wong BC, Zhang L, Ma JL, Pan KF, Li JY, Shen L, et al. Effects of selective COX-2 inhibitor and Helicobacter pylori eradication on precancerous gastric lesions. Gut. 2012;61(6):812–8.
6. Sheh A, Fox JG. The role of the Gastrointestinal Microbiome in Helicobacter pylori pathogenesis. Gut Microbes. 2013;4(6):505–31.
7. Amieva M, Peek RM. Jr. Pathobiology of Helicobacter pylori-Induced gastric cancer. Gastroenterology. 2016;150(1):64–78.
8. Roviello G, Iannone LF, Bersanelli M, Mini E, Catalano M. The gut Microbiome and efficacy of cancer immunotherapy. Pharmacol Ther. 2022;231:107973.
9. Beura LK, Hamilton SE, Bi K, Schenkel JM, Odumade OA, Casey KA, et al. Normalizing the environment recapitulates adult human immune traits in laboratory mice. Nature. 2016;532(7600):512–6.
10. Sethi V, Vitiello GA, Saxena D, Miller G, Dudeja V. The role of the Microbiome in Immunologic development and its implication for pancreatic cancer immunotherapy. Gastroenterology. 2019;156(7):2097–e1152.
11. Binnewies M, Roberts EW, Kersten K, Chan V, Fearon DF, Merad M, et al. Understanding the tumor immune microenvironment (TIME) for effective therapy. Nat Med. 2018;24(5):541–50.
12. Montalban-Arques A, Katkeviciute E, Busenhart P, Bircher A, Wirbel J, Zeller G, et al. Commensal clostridiales strains mediate effective anti-cancer immune response against solid tumors. Cell Host Microbe. 2021;29(10):1573–e887.
13. Vétizou M, Pitt JM, Daillère R, Lepage P, Waldschmitt N, Flament C, et al. Anticancer immunotherapy by CTLA-4 Blockade relies on the gut microbiota. Volume 350. New York, NY: Science; 2015. pp. 1079–84. 6264.
14. Meimarakis G, Winter H, Assmann I, Kopp R, Lehn N, Kist M, et al. Helicobacter pylori as a prognostic indicator after curative resection of gastric carcinoma: a prospective study. Lancet Oncol. 2006;7(3):211–22.
15. Koizumi Y, Ahmad S, Ikeda M, Yashima-Abo A, Espina G, Sugimoto R, et al. Helicobacter pylori modulated host immunity in gastric cancer patients with S-1 adjuvant chemotherapy. J Natl Cancer Inst. 2022;114(8):1149–58.
16. Ni J, Wang M, Wang T, Yan C, Ren C, Li G, et al. Construction and evaluation of a polygenic hazard score for prognostic assessment in localized gastric cancer. Fundam Res. 2024;4(5):1331–8.
17. Kaech SM, Cui W. Transcriptional control of effector and memory CD8 + T cell differentiation. Nat Rev Immunol. 2012;12(11):749–61.
18. Weichselbaum RR, Ishwaran H, Yoon T, Nuyten DS, Baker SW, Khodarev N, et al. An interferon-related gene signature for DNA damage resistance is a predictive marker for chemotherapy and radiation for breast cancer. Proc Natl Acad Sci USA. 2008;105(47):18490–5.
19. Flament H, Rouland M, Beaudoin L, Toubal A, Bertrand L, Lebourgeois S, et al. Outcome of SARS-CoV-2 infection is linked to MAIT cell activation and cytotoxicity. Nat Immunol. 2021;22(3):322–35.
20. Legoux F, Salou M, Lantz O. MAIT cell development and functions: the microbial connection. Immunity. 2020;53(4):710–23.
21. Kumar BV, Ma W, Miron M, Granot T, Guyer RS, Carpenter DJ, et al. Human Tissue-Resident memory T cells are defined by core transcriptional and functional signatures in lymphoid and mucosal sites. Cell Rep. 2017;20(12):2921–34.
22. Poch T, Krause J, Casar C, Liwinski T, Glau L, Kaufmann M, et al. Single-cell atlas of hepatic T cells reveals expansion of liver-resident naive-like CD4(+) T cells in primary sclerosing cholangitis. J Hepatol. 2021;75(2):414–23.
23. Walker LJ, Kang YH, Smith MO, Tharmalingham H, Ramamurthy N, Fleming VM, et al. Human MAIT and CD8αα cells develop from a pool of type-17 precommitted CD8 + T cells. Blood. 2012;119(2):422–33.
24. Wang T, Shen Y, Luyten S, Yang Y, Jiang X. Tissue-resident memory CD8(+) T cells in cancer immunology and immunotherapy. Pharmacol Res. 2020;159:104876.
25. Kang SY, Han JH, Ahn MS, Lee HW, Jeong SH, Park JS, et al. Helicobacter pylori infection as an independent prognostic factor for locally advanced gastric cancer patients treated with adjuvant chemotherapy after curative resection. Int J Cancer. 2012;130(4):948–58.
26. Marrelli D, Pedrazzani C, Berardi A, Corso G, Neri A, Garosi L, et al. Negative Helicobacter pylori status is associated with poor prognosis in patients with gastric cancer. Cancer. 2009;115(10):2071–80.
27. Wang F, Sun G, Zou Y, Zhong F, Ma T, Li X. Protective role of Helicobacter pylori infection in prognosis of gastric cancer: evidence from 2,454 patients with gastric cancer. PLoS ONE. 2013;8(5):e62440.
28. Joshi SS, Badgwell BD. Current treatment and recent progress in gastric cancer. Cancer J Clin. 2021;71(3):264–79.
29. Karkhah A, Ebrahimpour S, Rostamtabar M, Koppolu V, Darvish S, Vasigala VKR, et al. Helicobacter pylori evasion strategies of the host innate and adaptive immune responses to survive and develop Gastrointestinal diseases. Microbiol Res. 2019;218:49–57.
30. Chaturvedi R, de Sablet T, Coburn LA, Gobert AP, Wilson KT. Arginine and polyamines in Helicobacter pylori-induced immune dysregulation and gastric carcinogenesis. Amino Acids. 2012;42(2–3):627–40.
31. Capitani N, Codolo G, Vallese F, Minervini G, Grassi A, Cianchi F, et al. The lipoprotein HP1454 of Helicobacter pylori regulates T-cell response by shaping T-cell receptor signalling. Cell Microbiol. 2019;21(5):e13006.
32. Chen L, Li B, Yang WC, He JL, Li NY, Hu J, et al. A dominant CD4(+) T-cell response to Helicobacter pylori reduces risk for gastric disease in humans. Gastroenterology. 2013;144(3):591–600.
33. Stevanović S, Pasetto A, Helman SR, Gartner JJ, Prickett TD, Howie B, et al. Landscape of Immunogenic tumor antigens in successful immunotherapy of virally induced epithelial cancer. Sci (New York NY). 2017;356(6334):200–5.
34. Barrozo RM, Hansen LM, Lam AM, Skoog EC, Martin ME, Cai LP, et al. CagY is an Immune-Sensitive regulator of the Helicobacter pylori type IV secretion system. Gastroenterology. 2016;151(6):1164–e753.
35. Philip M, Schietinger A. CD8(+) T cell differentiation and dysfunction in cancer. Nat Rev Immunol. 2022;22(4):209–23.
36. Sharma P, Allison JP. Dissecting the mechanisms of immune checkpoint therapy. Nat Rev Immunol. 2020;20(2):75–6.
37. Leko V, Rosenberg SA. Identifying and targeting human tumor antigens for T Cell-Based immunotherapy of solid tumors. Cancer Cell. 2020;38(4):454–72.
38. Bandey IN, Adolacion JRT, Romain G, Paniagua MM, An X, Saeedi A et al. Designed improvement to T-cell immunotherapy by multidimensional single cell profiling. J Immunother Cancer. 2021;9(3).
39. Mann TH, Kaech SM. Tick-TOX, it's time for T cell exhaustion. Nat Immunol. 2019;20(9):1092–4.
40. Han C, Yan P, He T, Cheng J, Zheng W, Zheng LT et al. PHLDA1 promotes microglia-mediated neuroinflammation via regulating K63-linked ubiquitination of TRAF6. Brain, behavior, and immunity. 2020;88:640–53.
41. Zhang M, Hu S, Min M, Ni Y, Lu Z, Sun X, et al. Dissecting transcriptional heterogeneity in primary gastric adenocarcinoma by single cell RNA sequencing. Gut. 2021;70(3):464–75.
42. Savas P, Virassamy B, Ye C, Salim A, Mintoff CP, Caramia F, et al. Single-cell profiling of breast cancer T cells reveals a tissue-resident memory subset associated with improved prognosis. Nat Med. 2018;24(7):986–93.
43. Clarke J, Panwar B, Madrigal A, Singh D, Gujar R, Wood O, et al. Single-cell transcriptomic analysis of tissue-resident memory T cells in human lung cancer. J Exp Med. 2019;216(9):2128–49.
44. Molodtsov AK, Khatwani N, Vella JL, Lewis KA, Zhao Y, Han J, et al. Resident memory CD8(+) T cells in regional lymph nodes mediate immunity to metastatic melanoma. Immunity. 2021;54(9):2117–e327.
45. Kok L, Masopust D, Schumacher TN. The precursors of CD8(+) tissue resident memory T cells: from lymphoid organs to infected tissues. Nat Rev Immunol. 2022;22(5):283–93.
46. Hayward SL, Scharer CD, Cartwright EK, Takamura S, Li ZT, Boss JM, et al. Environmental cues regulate epigenetic reprogramming of airway-resident memory CD8(+) T cells. Nat Immunol. 2020;21(3):309–20.
47. Zaiss DMW, Gause WC, Osborne LC, Artis D. Emerging functions of Amphiregulin in orchestrating immunity, inflammation, and tissue repair. Immunity. 2015;42(2):216–26.
48. Kofler DM, Marson A, Dominguez-Villar M, Xiao S, Kuchroo VK, Hafler DA. Decreased RORC-dependent Silencing of prostaglandin receptor EP2 induces autoimmune Th17 cells. J Clin Investig. 2014;124(6):2513–22.
49. Jiang J, Dingledine R. Role of prostaglandin receptor EP2 in the regulations of cancer cell proliferation, invasion, and inflammation. J Pharmacol Exp Ther. 2013;344(2):360–7.

Publisher's note